Structural Health Monitoring of Lightweight Structures by Use of Lamb Waves

Rolf LAMMERING*, Artem EREMIN**, Mirco N. NEUMANN*,
Ulrich GABBERT***, Seyed M. H. HOSSEINI***
*Institut für Mechanik, Helmut-Schmidt-Universität/Universität der Bundeswehr Hamburg
Holstenhofweg 85, 22043 Hamburg, Germany
**Deptartment of Applied Mathematics, Kuban State University
Ul. Stavropolskaya, Krasnodar, Russia
***Institut für Mechanik, Otto-von-Guericke-Universität Magdeburg
Universitätsplatz 2, 39016 Magdeburg, Germany

Abstract. In the experimental part of this work, the excitation and propagation of Lamb waves in carbon fiber reinforced composite plates is presented by visualized experimental data. Lamb waves are easily excited by thin piezoelectric patches adhered to the surface of the structure. Their propagation is observed experimentally by Scanning Laser Vibrometry. Results from Lamb wave reflection and mode conversion at damage locations are shown indicating the potential and the restrictions of the inspection method. In the numerical part of this work, honeycomb sandwich panels are considered which are also frequently used as lightweight structures due to their high stiffness. Because of their complex build-up the understanding of Lamb wave generation and propagation is much more difficult than in the case of conventional composite plates. Therefore, finite element simulations have been performed to study guided waves at different frequency ranges and in sandwich panels with different build-ups. The honeycomb panel has been modeled by an orthotropic layered plate as well as by a more complex model which takes into account the effective build-up. For the orthotropic plate model the core material parameters have been obtained from a numerical homogenization method. The influence of the build-up and of the applied frequency on the wave propagation will be discussed.

Introduction

Since a considerably amount of life cycle costs is due to inspection and repair and since damage can lead to catastrophic failure lightweight aerospace structures require advanced monitoring and inspection techniques. Because of to the increasing integration of fiber reinforced plastics which show specific damage characteristics, techniques based on elastic waves may play an increasing role for damage detection. In plate and shell structures, especially high frequency guided waves, i.e. Lamb waves, and their possible contributions to structural health monitoring methods are in the focus of current research. Reflections, refractions or mode conversions are distinct indications of faults or defects and are often instantaneous visible in the pattern of an otherwise undisturbed propagating wave. On the other hand, even conventional build-ups of composite plates make the interpretation of the signals difficult as will be demonstrated by experimental as well as numerical examples in this work.

First, anisotropic carbon fiber reinforced plates are investigated experimentally. The propagation of symmetric and antsymmetric Lamb waves is shown by pictures captured by

Scanning Laser Vibrometry. Furthermore, it is shown, how the damage location influences the pattern of the wave reflection. Secondly, a honeycomb plate is analyzed numerically. It will be demonstrated that its build-up as well as the excitation frequency are responsible for the way of wave propagation and thus for the signals which are captured by piezoelectric sensors adhered to the outer surfaces.

Before the presentation of the experimental and theoretical results, a short introduction into the propagation of elastic waves in anisotropic solids is given.

1. Waves in Anisotropic Solids

In the analysis of wave motion in anisotropic elastic media the well known Lamé-Navier equations for isotropic material have to be adjusted to the more general constitutive equation. The resulting equations may be considered as the local formulation of the balance of momentum in which Hooke's law has been introduced in order to replace the stresses by displacement derivatives. In the case of an anisotropic material one obtains

$$\frac{1}{2} C_{ijkl} (u_{k,lj} + u_{l,kj}) = \rho \ddot{u}_i \quad . \tag{1}$$

This equation may be rewritten alternatively as

$$\frac{1}{2} \mathbb{C} : grad\,(grad\,\mathbf{u} + grad^T\,\mathbf{u}) = \rho \ddot{\mathbf{u}} \tag{2}$$

In equations (1) and (2) C_{ijkl} respective $\mathbb{C}$ denotes the 4th order tensor of elasticity, u_i respective **u** represents the displacement field and ρ is the material density. In equation (1) an index separated by a comma indicates differentiation with respect to the designated coordinate and a superimposed dot with respect to time. In equation (2) bold quantities denote vectors. Solutions of these coupled, linear differential equations are given e.g. in [4].

The resulting eigenvalue problem yields three real positive solutions which are the velocities of the bulk waves in an infinite three-dimensional anisotropic solid. These bulk waves are non-dispersive. In the case of an isotropic solid, these three velocities are corresponding to the longitudinal wave (P-wave), the vertically polarized shear wave (SV-wave), and the horizontally polarized shear wave (SH-wave). Since the velocities of the SV- and the SH-wave are the same for isotropic materials, only two distinct velocities remain in this case. For anisotropic materials, three distinct velocities are computed whose magnitude depend on the direction of propagation of the plane wave.

In the case of elastic plate and shell structures, the Lamé-Navier equations (1) and (2) are solved with respect to the respective boundary conditions, e.g. given stresses or displacements on the upper and lower surfaces. The analysis leads to the phenomenon of mode conversion that occurs when waves encounter a free boundary. This means that in the case of an incident P- or SV-wave, both a P-wave as well as an SV-wave may be reflected. So, the formation of Lamb waves may be considered as a consequence of P- and SV- wave reflections at the surfaces of plates and shells and the existence of two parallel free surfaces entails a new type of wave, so-called Lamb waves or guided plate waves. In contrast to the unbounded elastic media an infinite number of waves may emerge in plates and shells as can be seen from the related dispersion diagram. In Figure 1, left hand side, a dispersion diagram is presented for aluminium plates. The dispersive character of Lamb waves is clearly visible. Many textbooks, e.g. [2] or [1], deal with the Lamb wave theory.

In the case of an anisotropic laminate, the stiffness of the plate is depending on the direction under consideration. Thus, the phase velocities become direction dependent as can

be seen also from Figure 1, right hand side, cf. [5]. This effect will be under consideration in the next Section.

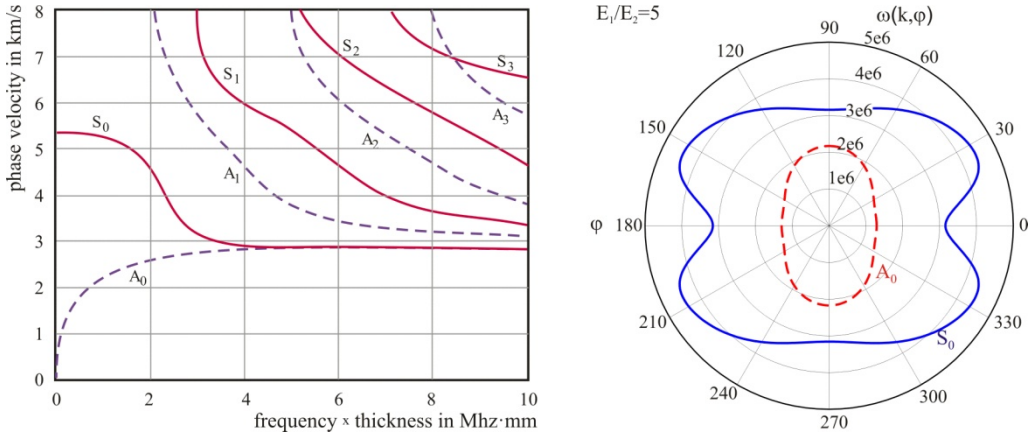

Figure 1: Left: Dispersion diagram of an aluminum plate. Right: Direction dependent phase velocities in a composite plate with stiffness ratio $E_1/E_2=5$, after [5].

1. Experimental Investigations on Lamb Waves in Orthotropic Plates

1.1 Experimental Set-Up

In the experimental part of this work, the Scanning Laser Vibrometry (SLV) is applied in order to investigate wave propagation in plate structures. A survey of laser vibrometry is given in [6].

Hardware components and software of the PSV-400-M Scanning Vibrometer (Polytec) are used in the following investigations. In this equipment, a He-Ne laser with a wavelength of $633 \cdot 10^{-9}$ *m* is used. As indicated by the denomination, a scan grid has to be defined which may comprise several ten thousand points. The scan grid may cover areas of various sizes. It is important that the amount of light scattered back from the different surfaces is sufficient for further signal analysis. In order to improve the reflectivity of a surface a retro-reflective tape or paint may be used. The hardware components are complemented by a software package that controls the scanner, the data processing, and the visualization of the measurement results.

Two carbon fiber composite plates (*1000 mm* × *1000 mm*) of *app. 2.2 mm* thickness serve as a test specimens. Each of them consists of 4 layers. The stacking sequence is [0, 0, 0, 0] (unidirectional fibers) and [0, 90, 90, 0] (cross ply laminate). A thin circular piezo-electric ceramic is adhered to the outer surface and serves as an actuator. The investigations are performed with the help of two powerful magnets (*5 mm* cubes) which have been placed opposite to each other at both sides of the plate at different locations. These magnets cause an effect which can be considered as structural disturbance or artificial damage.

Depending on the frequency different Lamb modes can be generated as it can be seen from the dispersion diagram, cf. Figure 1. In the following investigations, a five cycle sine burst at 70 *kHz* filtered by a Hann window is used as an excitation signal of the *S0*- and the *A0*-modes. In preceding analytical investigations and preliminary tests, this kind of signal has turned out to be advantageous with respect to the specimens, the mounted actuators, and the artificial damage.

1.2 Results and Discussion

Figure 2 shows the displacement field at the top of the carbon fiber reinforced plastic plate with [0, 0, 0, 0] stacking sequence (unidirectional fiber orientation). The white circle in the center of the pictures is excluded from scanning because the actuator is located here and would have disturbed a proper resolution of the propagating wave field. The fibers are aligned horizontally, so the phase velocity is higher in the horizontal direction than in the vertical one.

In the following, the left and the center pictures are under discussion. In the outer region of the left picture, the S0-mode is still visible while in the inner region, the A0-mode can clearly be detected. Furthermore, the left picture depicts sharply the location of the magnets which are located at the right side of the actuator in fiber direction. They may be considered as an artificial defect which becomes the source of a reflected *A0*-wave when it is reached by the propagating *A0*-wave. This figure already shows that the pattern of the reflected wave is similar to the pattern of the originally generated waves. The picture in the center emphasizes this fact and visualizes clearly the affinity of the ellipses. It should be noted, that both pictures are scaled in the same way, i.e. the brightness of the colours indicate the magnitude of the out of plane displacement. So, the attenuation of the amplitude from the left to the center picture becomes apparent.

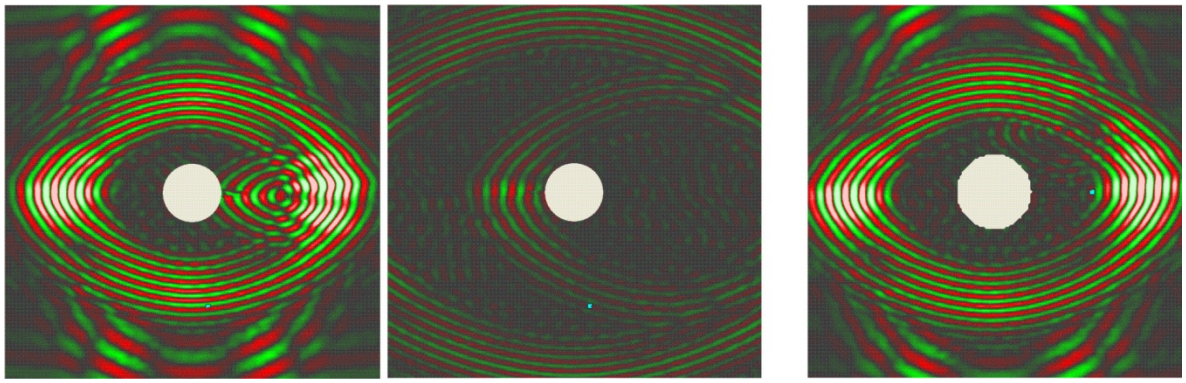

Figure 2: Wave propagation in carbon fiber reinforced plastic plate
with stacking sequence [0, 0, 0, 0] (unidirectional fibers) and with artificial defect.
Left and center: Magnets right from the center in fiber direction. Right: Magnets top right from the center.

The situation becomes different, when the magnets are not located directly in fiber direction (horizontally away from the center), but at a top right position, cf. Figure 2, right picture. The incident *A0*-wave is also reflected at the magnets, but the reflected *A0*-wave is less clearly visible. It should be mentioned, that the left and the right pictures in Figure 2 are taken at nearly the same time as can be seen from the front of the generated *A0*-wave. Due to the weakly developed reflected wave, it is nearly not noticeable anymore at a later time.

It should be noted that the artificial damage becomes clearly visible due to the reflection of the *A0*-mode in these experiments. The reflection of the *S0*-mode is less developed and worse detectable. Of course, this result has to be verified in the presence of a real damage, e.g. a delamination.

The second example is concerned with a specimen with [0, 90, 90, 0] stacking sequence (cross ply laminate). The experiments with this specimen are the same as described above. The results are shown in Figure 3.

The left picture in Figure 3 shows clearly the propagating *A0*-mode. It becomes clear that due to the fiber reinforcements which are in the vertical and horizontal directions now the shape of the wave front is more round bodied compared to the respective situation

in Figure 2. Furthermore, the location of the magnets right from the actuator is easy to detect since the so produced artificial damage is the source of the reflected wave. Again, the affinity of the reflected wave pattern and the pattern of the originally generated waves is obvious. This fact is also shown by the center picture which shows the same experiment at a later time. The attenuation of the out-of-plane amplitude is observed again by the decreasing brightness.

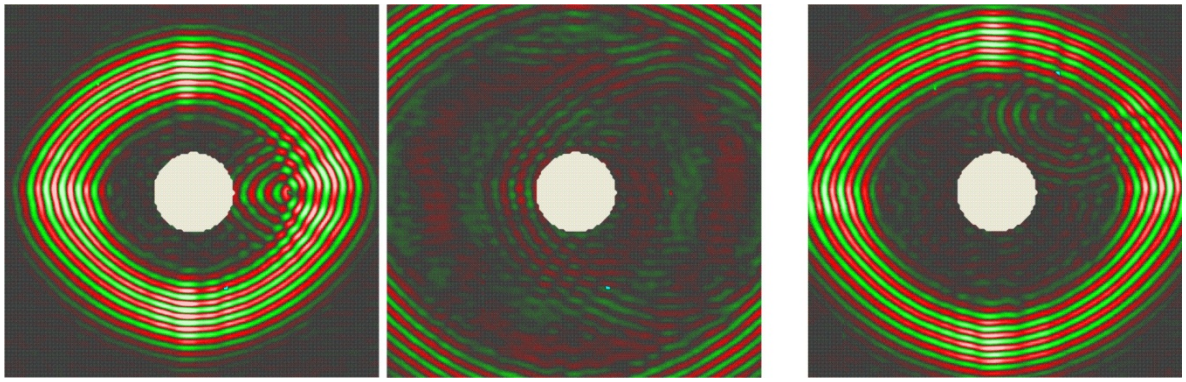

Figure 3: Wave propagation in carbon fiber reinforced plastic plate
with stacking sequence [0, 90, 90, 0] (cross ply laminate) and with artificial defect.
Left and center: Magnets right from the center in fiber direction. Right: Magnets top right from the center.

In the right picture of Figure 3 the magnets are located again top right from the actuator so that the fibers are not aligned to the actuator-magnet direction. The reflected wave is clearly visible so that it can be found out that the pattern of the reflected wave does not agree with the pattern of the originally generated waves.

Altogether, the above presented results of wave propagation and wave reflection in fiber reinforced plastic plates show definitely that damage detection in anisotropic plates is extremely complicated and much more complex than in isotropic structures. Especially damage detection which is not based on fully two-dimensional information but on a sensor network is a challenging task. On the other hand, the necessity for mathematical models and numerical analysis is apparent. This is in the focus of the next Section.

3. Analysis of Lamb Wave Propagation in Honeycomb Sandwich Panels

3.1 Finite Element Modeling

In the numerical part of this work, a sandwich plate is under investigation. It is consisting of two outer plate layers, a honey comb core material in between, and piezoelectric actuators and sensors at the outer surfaces. The related finite element model is composed from 3-D solid elements for the plates, 2-D solid shell elements for the honeycomb cells and 3-D piezoelectric elements for the PZT actuator/sensor, respectively. In addition, in a simplified model, 3-D solid elements with orthotropic material properties are used for the core material. The material properties of the elements are calculated using a homogenization technique. Two sensors are placed on the top and bottom layers in opposite to each other in order to capture the signals on both sides of the sandwich panel. The distance between the actuator and the sensors is *180 mm*. The x-direction points from the actuator to the sensors. A zero voltage is applied to the bottom surfaces of the sensors and actuator (the side attached to the panel) and the exciting signal of half-cycle narrow band tone burst [7] is applied to the top nodes of the actuator:

$$V_{in}(t) = V\left\{H(t) - H(t - \frac{3.5}{f_c})\right\}\left\{1 - \cos\frac{2\pi f_c t}{3.5}\right\}\sin 2\pi f_c t \qquad (3)$$

Here, t is the time, f_c is the central frequency and $H(t)$ is the Heaviside step function. The signal of the piezoelectric sensors is calculated from the nodal voltages of the top nodes. In order to model the conductivity of the copper layer on the top of the sensor correctly, all nodes lying there are tied together. The wave reflections at the free boundaries are reduced by a non-reflecting boundary condition, cf. [3]. The damping capability of the elements is increased gradually from zero to high values at the free edges, using an exponential function.

Table 1: Geometrical properties of the sandwich panel in cases (1) and (2)

Skin plate		Honeycomb cell, [7]		PZT actuator/sensor, [7]	
Length (mm)	Width (mm)	Cell size (mm)	Height (mm)	Radius (mm)	Thickness (mm)
290	124	4.8	15	3.17	0.7

Table 2: Material properties of the plate and the honeycomb cells.

Skin plate (Aluminium alloy T6061, [7])					
Young's modulus (GPa)		Poisson's ratio (-)		Density (kg m^{-3})	
2700		0.33		2700	
Honeycomb cell (HRH-36-1/8-3.0)					
$E_x = E_x$ (GPa)	E_z (GPa)	ν_{xy} and $\nu_{yz} = \nu_{xz}$ (-)	G_{xy} (GPa)	$G_{xy} = G_{xz}$ (GPa)	Density (kg m^{-3})
2.46	3.4	0.3	0.94615	1.154	50

In this study two different honeycomb sandwich panels with different geometrical properties are considered. In the first case a sandwich panel with 2 *mm* plate thickness and a honeycomb thickness of 0.22 *mm* is considered (case (1)), and in the second case a sandwich panel with a plate thickness of 0.5 *mm* and a honeycomb thickness of 1.48 *mm* has been modeled (case (2)). Some more geometrical properties are shown in Tab. 1. In addition, Tab. 2 shows the material properties of the plates and the honeycomb core materials. The material properties of the PZT actuator/sensor are presented in [7].

All simulations are performed with the commercial finite element package MSC.Marc® (MSC Software Corporation, Santa Ana, CA, USA).

3.2 Signal Analysis

To determine the group velocity dispersion curves of the propagated waves on the surfaces, the continuous wavelet transform (CWT) based on the Daubechies wavelet D10 is used, cf. [7] and [8].

3.3 Results and Discussion

Figure 4 is a snapshot of the wave field u_z in the sandwich panel. When the central frequency of the exciting signal is relatively low (*5 kHz*), it can be seen, that the wave length in case (1) is longer than in case (2), see Figure 4, upper left and right pictures. It must be mentioned, that in case (1) the wall thickness of the honeycomb cell is thinner compared to case (2). In the case of relatively high central frequencies *(100 kHz)* of the exciting signal the wave propagates mostly on the top plate in case (1), where the actuator is attached, see Figure 4, lower left picture. However, for the same exciting signal in the case (2) the wave propagation can also be observed on the opposite side of the actuator, see Figure 4, lower right picture. This can be explained by the fact that the thickness of the skin plate in the model case (1) is thicker than in model case (2).

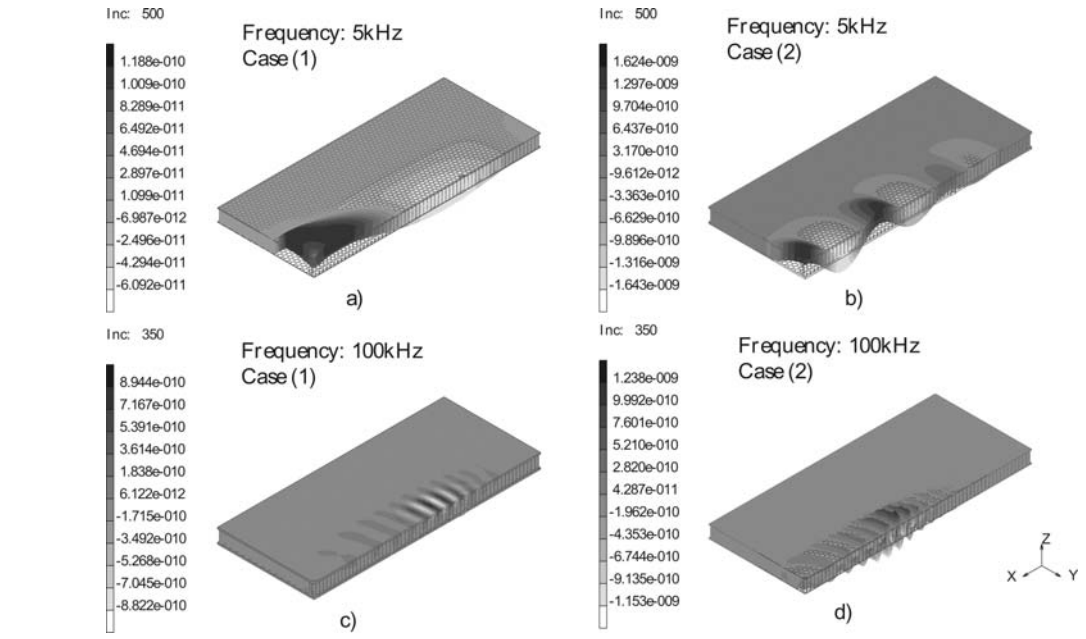

Figure 4: The wave field u_z in a sandwich panel structure at central frequencies of 5 and 100 kHz.
Case (1): 2mm plate thickness and 0.22mm core thickness;
Case (2): 0.5mm plate thickness and 1.48mm core thickness.

The sensor signals captured on the top surface of the sandwich panel are shown in Figure 5. The results are derived from a real honeycomb sandwich panel (real), a sandwich panel with homogenized core (homo) and a single plate (plate).

For the case (1) model (thick plates, thin core) the signals captured from the real and the homogenized models agree well all together. However, at lower frequencies, the signals from the single plate do not match with the signals of the real and the homogenized models. But with increasing excitation frequency a better agreement is observed between all models. This can be explained by the fact that for a high frequency excitation the wave propagates mostly on the top plate in the case (1) model. It should be mentioned here that the periodicity of the honeycomb is only included in the detailed model (real) which therefore should be considered as a reference model.

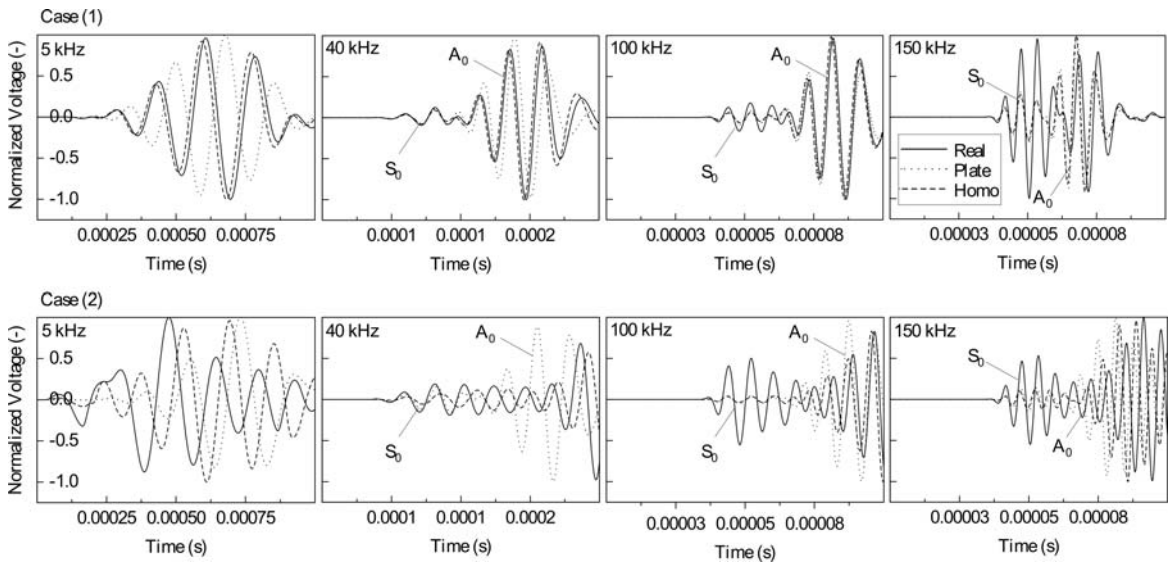

Figure 5: Sensor signals on the top layer at different central frequencies. Comparison of three models: (real): real geometry of the honeycomb sandwich panel; (homo): sandwich panel with homogenized core; (plate): single plate. Case (1) and (2) refer to different sandwich panel geometries, cf. Figure 4.

For the case (2) model (thin plates, thick core) the different models do not show consistent results in the low frequency range. With increasing frequency, the symmetric modes (S0) are in rather good agreement; however, this is not the case for the antisymmetric modes (A0). The reason of this dynamic behavior may be that the honeycomb core plays a more important role than in the case (1) model so that it has to be modelled properly without simplifications of a homogenization process.

4. Conclusions and Outlook

The experimental as well as the theoretical investigations in this work are showing the more complex physics of wave propagation and wave reflection in anisotropic plates as well as in sandwich structures compared to isotropic media. Moreover, the experimental investigations emphasize that elastic waves are a suitable means for damage detection. However, anisotropy has to be incorporated into models which have to be developed. Furthermore, damping has to be taken into account for these models. The numerical investigations on sandwich structures show the strong influence of the build-up and of the test parameters, such as the frequency. Future numerical investigations will include the effect of damage.

Acknowledgements

The financial support of the *Deutsche Forschungsgemeinschaft* (DFG) is gratefully acknowledged (PAK 357). Furthermore, the authors express their thanks to the *Deutscher Akademischer Austauschdienst* (DAAD) for supporting the cooperation with Kuban State University.

References

[1] J. Achenbach: *Wave Propagation in Elastic Solids*. North Holland, 1973.
[2] K. F. Graff: *Wave Motion in Elastic Solids*. Clarendon Press, 1975
[3] G. R. Liu and S. S. Quek Jerry: A non-reflecting boundary for analyzing wave propagation using the finite element method. *Finite Elem. Anal. Des.*, 39, 403-417, 2003.
[4] G.R. Liu; Z.C. Xi: *Elastic Waves in Anisotropic Laminates.* CRC Press, 2002.
[5] F. Schöpfer, F. Binder, A. Wöstehoff, and T. Schuster: A Mathematical Analysis of the Strip-Element Method for the Computation of Dispersion Curves of Guided Waves in Anisotropic Layered Media, *Mathematical Problems in Engineering,* Vol. 2010, Article ID 924504, doi:10.1155/2010/924504, 2010.
[6] W. N. Sharpe: *Springer Handbook of Experimental Solid Mechanics*. Springer, 2008.
[7] F. Song, G. L. Huang and K. Hudson: Guided wave propagation in honeycomb sandwich structures using a piezoelectric actuator/sensor system. *Smart Mater. Struct.*, 18, 125007, 2009.
[8] A. Ungethüm and R. Lammering: Impact and Damage Localization on Carbon-Fibre Reinforced Plastic plates. In. F. Casciati and M. Giordano: Structural Health Monitoring 2010, 823-828. Proc. 5th Europ. Workshop on Structural Health Monitoring, Sorrento, Italy, June 28 – July 4, 2010.